Biotechnol Lett (2021) 43:1845–1867
https://doi.org/10.1007/s10529-021-03157-3

ORIGINAL RESEARCH PAPER

Infected insect gut reveals differentially expressed proteins for cellular redox, metal resistance and secretion system in *Yersinia enterocolitica-Helicoverpa armigera* pathogenic model

Shruti Ahlawat · Amarjeet Kumar Singh · Akshay Shankar · Asha Yadav · Krishna Kant Sharma

Received: 10 April 2021 / Accepted: 17 June 2021 / Published online: 24 June 2021
© The Author(s), under exclusive licence to Springer Nature B.V. 2021

Abstract

Objective Mouse infection models are frequently used to study the host–pathogen interaction studies. However, due to several constraints, there is an urgent need for a simple, rapid, easy to handle, inexpensive, and ethically acceptable in vivo model system for studying the virulence of enteropathogens. Thus, the present study was performed to develop the larvae of *Helicoverpa armigera* as a rapid-inexpensive in vivo model system to evaluate the effect of *Yersinia enterocolitica* strain 8081 on its midgut via a label-free proteomic approach.

Results *Helicoverpa armigera* larvae fed with *Yersinia enterocolitica* strain 8081 manifested significant reduction in body weight and damage in midgut. On performing label-free proteomic study, secretory systems, putative hemolysin, and two-component system emerged as the main pathogenic proteins. Further, proteome comparison between control and *Yersinia* added diet-fed (YADF) insects revealed altered cytoskeletal proteins in response to increased melanization (via a prophenoloxidase cascade) and free radical generation. In concurrence, FTIR-spectroscopy, and histopathological and biochemical analysis confirmed gut damage in YADF insects. Finally, the proteome data suggests that the mechanism of infection and the host response in *Y. enterocolitica-H. armigera* system mimics *Yersinia*-mammalian gut interactions.

Conclusions All data from current study collectively suggest that *H. armigera* larva can be considered as a potential in vivo model system for studying the enteropathogenic infection by *Y. enterocolitica* strain 8081.

Supplementary Information The online version contains supplementary material available at https://doi.org/10.1007/s10529-021-03157-3.

S. Ahlawat · A. Shankar · A. Yadav · K. K. Sharma (✉)
Laboratory of Enzymology and Recombinant DNA Technology, Department of Microbiology, Maharshi Dayanand University, Rohtak, Haryana 124001, India
e-mail: kekulsharma@gmail.com; kksharma.microbiology@mdurohtak.ac.in

A. K. Singh
Centre for Genetic Manipulation of Crop Plants, University of Delhi South Campus, Benito Juarez Road, New Delhi 110021, India

Graphic abstract

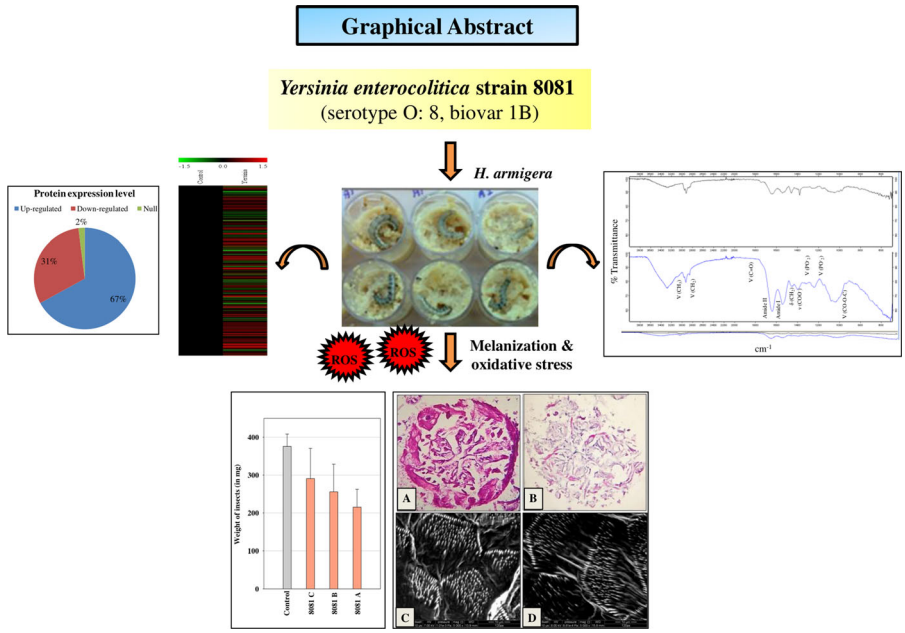

Keywords Proteomics · *Helicoverpa armigera* · *Yersinia enterocolitica* · Reactive oxygen species · Laccase · Secretion system

Introduction

Yersinia enterocolitica is a gram-negative, facultative anaerobic, non-sporulating, coccobacillary gamma-proteobacterium belonging to the family of Enterobacteriaceae (Rakin et al. 2015). It is a potential human pathogen with vast serotype diversity. It has been differentiated into 6 biovars viz., 1A, 1B, and 2–5 based on biochemical tests (Virdi et al. 2012; Singh et al. 2014), and greater than 70 serotypes depending on the antigenic variations in the O-antigen of the lipopolysaccharides (Rakin et al. 2015). *Y. enterocolitica* biovar 1B, a highly virulent biovar, is a food-borne and water-borne pathogen, but blood-transfusion associated septicemia and mortality is also reported. The enteropathogenic *Y. enterocolitica* invades the intestinal epithelium and multiplies in the lymphatic system (Ahlawat et al. 2020). The highly virulent strains of *Y. enterocolitica* subsp. *enterocolitica* posses a virulence plasmid (pYV), heat stable toxin (YstA), high-pathogenicity islands (HPI), chromosomally-encoded type II (T2SS) and type III (T3SS) secretion systems, resistance-gene loci, various metal-uptake operons (Thomson et al. 2006), genomic islands, prophages, putative hemolysins, adhesions, and low redox laccases (Singh et al. 2014, 2016; Ahlawat et al. 2020). *Yersinia* secretion locus of pYV plasmid encodes a T3SS along with a set of virulence factors, i.e., *Yersinia*-outer membrane proteins (Yops). The virulence factor T3SS of *Yersinia* inhibits its phagocytosis in host, while HPI has a role in siderophore yersiniabactin-mediated iron uptake (Rakin et al. 2015).

Conventionally, mouse infection models are used to study the pathology of *Y. enterocolitica* and other human pathogens. However, due to ethical concerns, limited number of animals can be used. Further, the experimental animals are costly and the maintenance of animal facilities is expensive. Therefore, there is an urgent need for a simple, rapid, easy to handle, inexpensive, and ethically acceptable in vivo model for studying the virulence of enteropathogens. Interestingly, *Y. enterocolitica*, which is considered as a mammalian pathogen, is also toxic to insects. *Yersinia* is toxic to *Manduca sexta* or tobacco hornworm. It also colonizes *Caenorhabditis elegans* by expanding its intestinal lumen and thus killing the nematode (Ahlawat et al. 2020). Further, *Galleria mellonella* or wax-

moth insect larva is a commonly used alternative infection model for enteropathogens (Alenizi et al. 2016) including *C. jejuni* (Senior et al. 2011) and *Klebsiella pneumoniae* (Insua et al. 2013). It is also used to assess the host–pathogen interactions (Hurst et al. 2015). The insect gut provides an alternate and analogous subject to the vertebrate gut, such as the alkaline pH of midgut, apical end of columnar cells in midgut is covered by short hair-like projections called microvilli, and digestive tract of insects is lined with an invertebrate-unique structure called peritrophic membrane (PM) (Zhang and Guo 2011), i.e., widely analogous to the mucous lining of the vertebrate gut (Campbell et al. 2008).

In an earlier work, a label-free quantitative proteomic technique was performed to gain insights into *Beauveria bassiana-Bombyx mori* interaction. According to this report, the screening of immune molecules against *B. bassiana* at the proteome level is more accurate and rapid than the screening at the transcriptome level (Lü et al. 2019). Another study based on a label-free proteomic method offers evidence for host defense against *B. mori* nuclear polyhedrosis virus (BmNPV) infection, thereby suggesting the potential function of insect midgut after oral infection (Zhang et al. 2019). Their short life cycle and no ethical constraints make them an ideal model system for evaluating the virulence of pathogens. Therefore, the current study was performed to develop the larvae of *H. armigera* (Hübner) (Lepidoptera: Noctuidae) as a rapid-inexpensive in vivo model system to evaluate the effect of an enteropathogen *Y. enterocolitica* strain 8081 (1B/O:8) on its midgut. Further, the entomopathogenic potential of *Y. enterocolitica* strain 8081 in the mid gut of *H. armigera* larvae was evaluated via a label-free proteomic approach, and validated through spectroscopic, biochemical, histopathology and microscopic studies.

Materials and methods

Materials

Guaiacol, isopropyl-β-D-1-thiogalactopyranoside (IPTG), and kanamycin were purchased from Sigma-Aldrich products, Merck KGaA, Darmstadt, Germany Inc., while all other media components were purchased from Hi-Media, Mumbai, India and were of reagent grade or better.

Bacterial strain preparation and *H. armigera* larval infection

The reference strain, i.e., *Y. enterocolitica* strain 8081 (1B/O:8) used in the present study is an American Type Culture Collection (ATCC) strain that was generously provided by Prof. J.S. Virdi, University of Delhi, South Campus, New Delhi, India. *Y. enterocolitica* strain 8081 (1B/O:8) was grown in LB medium at 37 °C, 200 rpm until stationary growth phase (OD_{600} is $\sim$ 1–5 $\times$ 10^9 colony forming unit (CFU)/mL). The cell pellet obtained by centrifuging cells at 5000 rpm, 10 min, and 4 °C was washed and suspended in normal saline. First-instar *H. armigera* neonate larvae were obtained from National Bureau of Agricultural Insect Resources (NBAIR) [Bangalore, India] and only healthy-looking larvae were used in the experiment. Two days old (first-instar) larvae of *H. armigera* were challenged orally with *Y. enterocolitica* strain 8081 [undiluted (10 µL/mL), 10^{-1} dilution, and 10^{-2} dilution] along with the artificial diet, till fourth-instar. The control insect larvae were fed with the artificial diet. The experiments were performed in several replicates with body weight, morbidity, and mortality in insect monitored and recorded. Thereafter, ten-day old (fourth-instar) larvae of both control and *Yersinia* added diet-fed (YADF) insects were dissected aseptically and the gut was excised for biochemical, histopathology, scanning electron microscopy (SEM), and label-free LC–MS/MS proteomic studies. The insect bioassays were performed at 27 ± 1 °C, RH 65 ± 5%, and 16 h light/8 h dark cycle for eight days [from two days old (first-instar) larvae to ten days old (fourth-instar) larvae]. Proteomic analysis was carried out on ten-day old (fourth-instar) larvae on the basis of morbidity data.

Statistical analysis of data

The data of insect weight was calculated as mean values [± standard deviation]. The statistical analysis was performed by one-way Analysis of Variance (ANOVA) using Microcal Origin 6.0 (Microcal Origin Software, Northampton, Massachusetts). The mean values obtained from each sample were compared by

using an unpaired *t*-test. A probability value < 0.05 was regarded as statistically significant.

Proteomic analysis of YADF insect gut

Protein preparation, digestion and nano-LC–MS/MS

The proteomic analysis of the excised gut of the YADF insects was performed as discussed in our previous reports (Ahlawat et al. 2020). The excised gut of the ten days old (fourth-instar) larvae were briefly sonicated in extraction buffer. After the breakdown of tissue the protein was precipitated using 8:1 (Acetone:TCA). The pellets obtained were washed by using dithiothreitol-acetone. Thereafter, the protein was solubilized and quantified using nanodrop, reduced, alkylated, and diluted by using 25 mM ABC (pH $\sim$ 7.0). The digestion was done by adding trypsin in 1:50 ratio and trypsinization was stopped by adding FA. Further, the samples were dried and reconstituted in FA. The digested peptides were analyzed using a nano LC–MS/MS. The peptides were loaded onto a 2 µm $\times$ 50 cm PepMap RSLC C_{18} pre-column and then eluted at 300 nL/min flow-rate by using a gradient of solution A and B for 123 min. The full-scan MS spectra (m/z 350–2000) were obtained on a Q-Exactive Orbitrap in a positive-ion mode (Jain et al. 2019).

Data analysis and bioinformatics studies

Raw mass spectrometry data files acquired from the mass spectrometer were handled using proteome discoverer software (ver. 2.2, Thermo Fisher Scientific, USA). The acquired MS files were searched against the database of protein sequence related to *Helicoverpa* and *Yersinia* available in UniProt (http://www.UniProt.org/). SEQUEST-HT results were filtered with the Percolator-based scoring to enhance the accuracy and sensitivity of the peptide identification. The proteins and peptides were deduced from spectrum identification results by using peptide spectrum matches (PSMs). Proteins and peptides were validated at a false discovery rate (FDR) of 0.1% assessed by using decoy-hit distribution. The proteins were selected by *q*-value (≤ 0.05) by using in-built statistical packages of proteome discoverer (ver. 2.2, Thermo Fisher Scientific, USA). The results were filtered by Xcorr (< 1.5), PSMs (≥ 5) for proteins and ΔCn (< 0.01) for peptides with a high confidence (Jain et al. 2019).

Protein quantification was done using the total MS/MS spectrum count of the identified proteins. Additional criteria were employed to enhance the confidence. Normalization of identified PSMs among LC–MS/MS runs was done by dividing individual PSMs of proteins by total PSMs and average of % PSM count was used for evaluating the fold-changes for treatment conditions, as described earlier (Ahlawat et al. 2020). For contrasting relative intensities of proteins between control and YADF insects groups, samples were assessed by using cumulative-confident-normalized PSMs value. Functional assignment and annotation by gene ontology (GO) terms (www.geneontology.org/), InterPro terms (InterProScan, EBI: https://www.ebi.ac.uk/), enzyme classification (EC) codes, and metabolic pathways (Kyoto Encyclopaedia of Gene and Genomes, KEGG) were determined by OmicsBox (https://www.biobam.com/omicsbox/) and Blast2GO (https://www.blast2go.com/). The heat map cluster was made using Multi Experiment Viewer (MeV) software suite (ver. 4.9; http://mev.tm4.org/) and protein–protein interaction networks (PPIs) were analyzed via Search Tool for the Retrieval of Interacting Genes/Proteins (STRING) software (ver. 11.0; https://string-db.org/). The mass spectrometry proteomics data have been deposited to the ProteomeXchange consortium via the proteomics identification database (PRIDE; https://www.ebi.ac.uk/pride/) (Perez-Riverol et al. 2019) partner repository with the dataset identifier PXD021304.

Effect of *Y. enterocolitica* infection on *H. armigera* larvae gut

Biochemical and spectroscopic studies

To study biochemical changes the gut homogenate was prepared from the excised ten days old (fourth-instar) larval gut. Catalase (CAT), an antioxidant enzyme, catalyzes the breakdown of hydrogen peroxide (H_2O_2) to less toxic products (Rajendran et al. 2014). Catalase assay was done according to the procedure described earlier (Cuéllar-Cruz et al. 2009). It measures the decomposition of H_2O_2 by enzyme catalase. One unit of catalase decomposes 1 µM of H_2O_2 per minute at 25 °C and pH 7 under the specified conditions. The amount of H_2O_2 decomposed was

calculated and the results were expressed as nmol of H_2O_2 decomposed/min/mg protein. Lipid peroxidation (LPO), defined as deterioration of membrane lipids by free radicals that result in the formation of stable oxidation products (Kurutas 2016), was assayed via the modified method of Wills (1966). The stable oxidation products of LPO are commonly used as the biomarkers of oxidative/nitrosative stress or damage and the results were expressed as nmol malondialdehyde (MDA)/mg protein. Glutathione (GSH) was estimated as described by Kumar et al. (2008). The results were expressed as µg glutathione/mg protein. GSH is an intracellular antioxidant that can accommodate the loss of a single electron due to the presence of sulfur containing thiol group (Kurutas 2016). Thereafter, Lowry's method was used to determine the protein concentrations, using bovine serum albumin (BSA) as a standard. Further, the ten days old (fourth-instar) larval gut samples were freeze-dried by using the lyophilizer (Allied Frost, India) and the change in structure was examined by performing the fourier-transform infra-red (FTIR) spectroscopy on a FTIR-5300 spectrophotometer (Alpha FTIR, Bruker, Germany) to record data in 500–4000 cm^{-1} scanning range.

Imaging studies of YADF insect gut

Aseptically excised ten days old (fourth-instar) larval gut samples were stored in 2% paraformaldehyde prior to histopathological analysis. Sections of larval gut tissue (10–15 µm) were sliced using CM3600 Cryomicrotome (Leica Microsystem Ltd., Germany) followed by fixation on a gelatin-coated slide. After fixation, the tissue samples were stained with hematoxylin and eosin (H-E). The gelatin-coated slides were dipped in hematoxylin for 1–5 min and washed with water for 5 min, followed by eosin staining for 25 s and washing. Further, the slides were dipped subsequently in 75%, 95%, and 100% ethanol for 1 min each, followed by xylene treatment for 3 min. Finally, the slides were DPX (dibutylphthalate polystyrene xylene) mounted and observed under the light microscope.

Scanning electron microscopy (SEM) was done commercially at Indian Institute of Technology (IIT), New Delhi, India. For SEM, the gut tissues of fourth-instar larvae were fixed in 2% paraformaldehyde and vacuum-dried. Dried tissues were mounted, coated with palladium, and examined using FEI Quanta 200F integrated with Oxford-EDS system (IE 250 X Max 80), Netherlands at 7 kV.

Results

Proteomic analysis of YADF insect gut

For performing label-free LC–MS/MS proteomic studies, two days old (first-instar) larvae of *H. armigera* were orally challenged with *Y. enterocolitica* strain 8081 in the artificial diet till fourth-instar. The insect bioassays were performed at 27 ± 1 °C, RH 65 ± 5%, and 16 h light/8 h dark cycle for eight days [from two days old (first-instar) larvae to ten days old (fourth-instar) larvae]. Thereafter, the ten days old (fourth-instar) larvae were dissected aseptically to obtain the excised gut tissues, which were pooled to perform the proteomic study. The experiments were performed using 22 control and 33 YADF insects larvae (11 each for 10^{-1}, 10^{-2}, and 10^{-3} dilution). Using label-free proteomic technique, i.e., Orbitrap nano-LC–MS/MS, a total of 1133 (306 exclusively in control insect larvae, 95 exclusively in YADF insects, and 732 shared between both the groups) unique protein accessions having PSM ≥ 1 were identified and quantified with a high confidence in this study (Fig. 1A).

Among all the identified proteins, about 2% were of *Yersinia* (Fig. 1B). The presence of *Yersinia* proteins in the insect gut tissues might be due to the establishment of *Y. enterocolitica* strain 8081 into the epithelial cells of the larvae gut, as the excised gut of *H. armigera* larvae was flushed with phosphate buffered saline (PBS) before performing the preliminary steps of proteomics. The *Yersinia*-identified proteins included metabolism proteins (13), transport and secretion proteins (2), putative hemolysins (1), secretory systems (2; T3SS:1, T6SS:1), and proteins for sensing, signaling, and regulation (4) (Supplementary Table 1).

GO annotation and KEGG pathway analysis of stringently-filtered insect proteins

On strict filtering of the dataset by using the criterion of PSMs ≥ 5, 467 proteins were stringently identified. Out of 467 proteins, 284 were shared between both

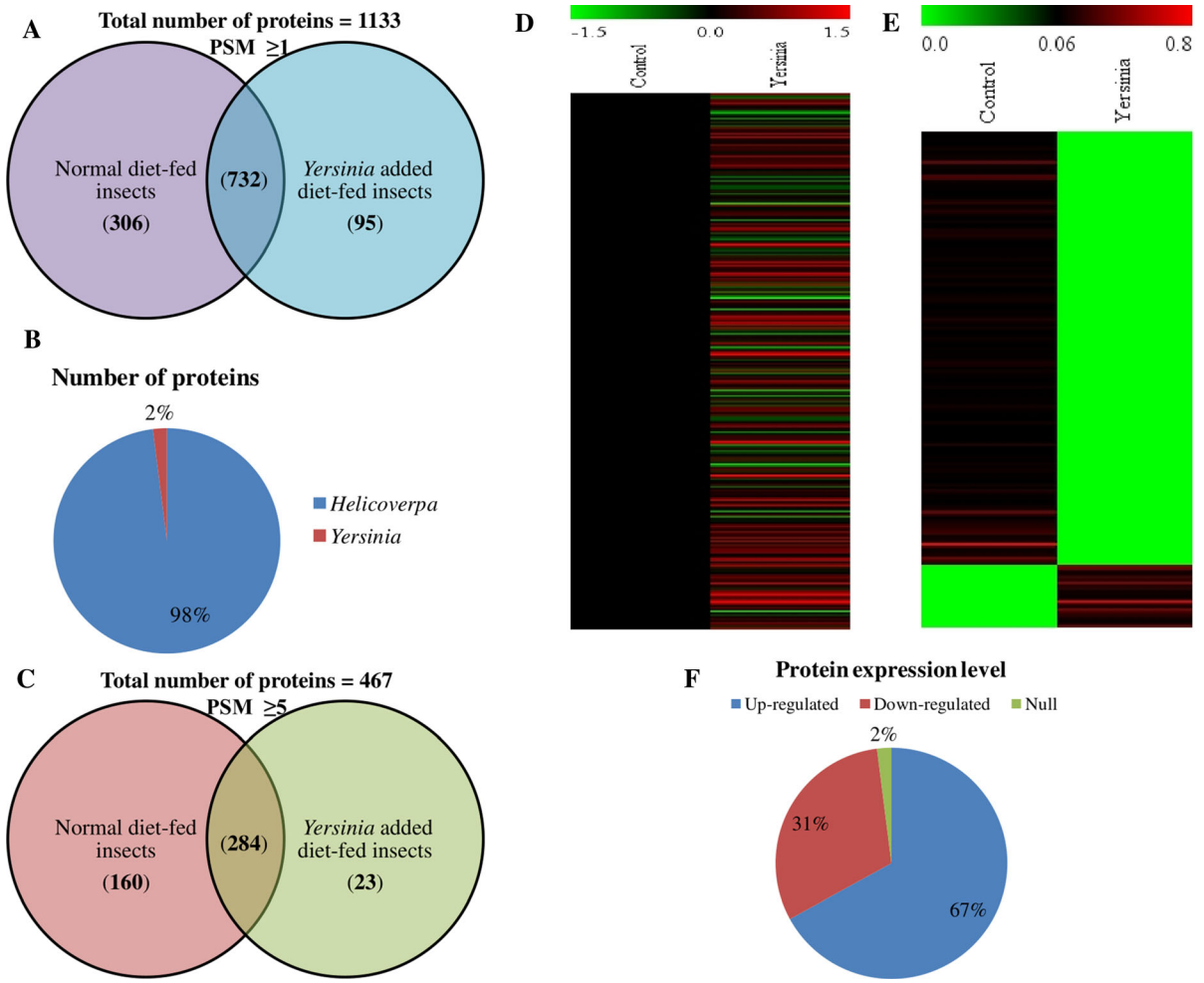

Fig. 1 **A** Distribution of 1133 identified protein accessions with PSMs ≥ 1, **B** Distribution of 1133 identified proteins accessions with PSMs ≥ 1 based on the match against protein sequences of *Helicoverpa* and *Yersinia* available in UniProt, **C** Distribution of 467 identified protein accessions with PSMs ≥ 5, **D** Heat map depicting changes in protein expression in *H. armigera* larvae with and without *Yersinia*-feeding using protein accessions common to both conditions, **E** Heat map depicting changes in protein expression in *H. armigera* larvae with and without *Yersinia*-feeding using protein accessions present in either group, **F** Distribution of 467 identified protein accessions with PSMs ≥ 5 based on expression levels

groups and 183 (160 in control, 23 in YADF insects) were exclusively determined in a single group (Fig. 1C). The differentially expressed proteins are shown in a heat map format by using normalized PSMs (Fig. 1D, E). The heat map data clearly indicate the diverse intensities (67% up-regulated, 31% down-regulated) of proteins between control and YADF insects (Fig. 1F). Further, identified proteins (467 proteins; PSMs ≥ 5) were classified based on biological process (BP), cellular component (CC), and molecular function (MF) categories in gene ontology (GO) annotations. GO analysis of control insects unique proteins displayed 37.51% BP, 10.77% CC, and 51.68% MF proteins. Comparatively, GO analysis of YADF insects unique proteins had 36.18% BP, 13.7% CC, and 50.1% MF proteins (Fig. 2, Supplementary Table 2). Further, when results of both the groups were compared, extracellular region (CC, GO: 0005576) and transferase activity (MF, GO: 0016740) classes or functions were reported to be unique in control insects. Biological regulation (BP, GO: 0065007), cytoskeleton (CC, GO: 0005856), and extracellular space (CC, GO: 0005615) classes or functions were unique in YADF insects (Fig. 2,

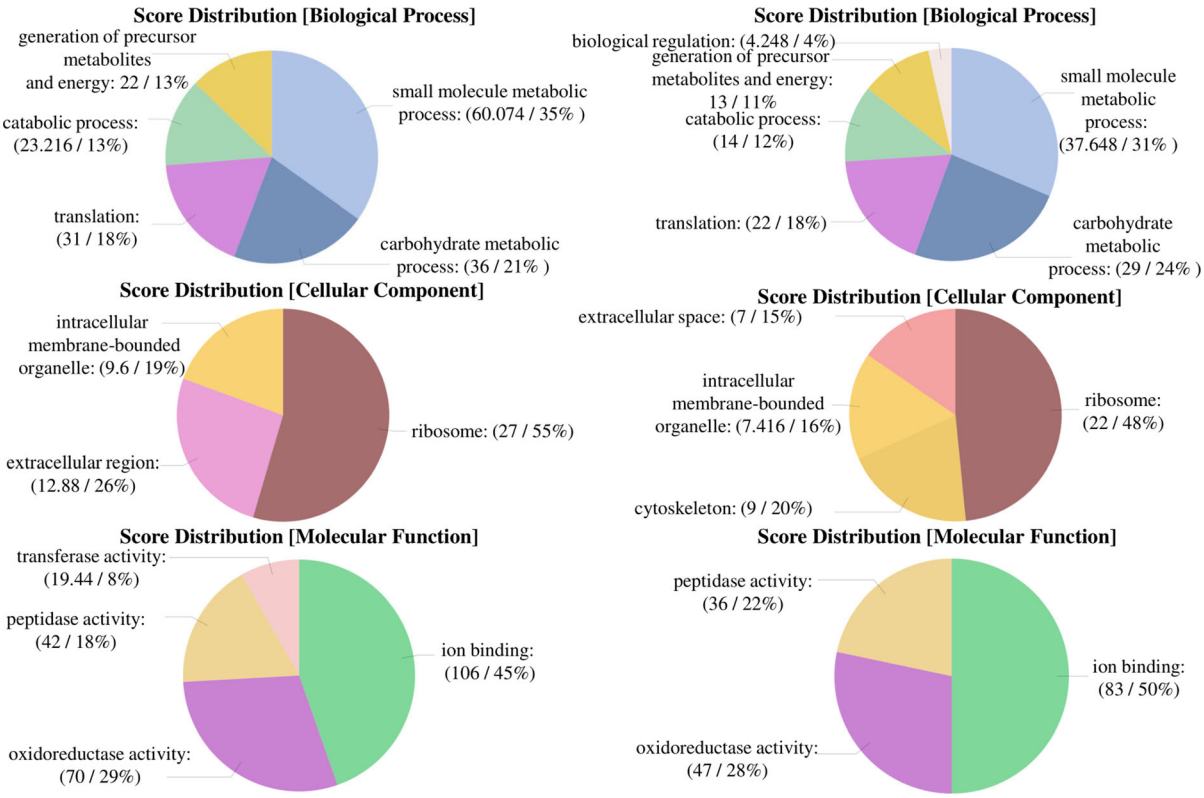

Fig. 2 Gene ontology (GO) analysis of differentially expressed protein accessions with PSMs ≥ 5 from normal diet-fed insects (on left) and YADF insects (on right)

Supplementary Table 3). A biological system employs a variety of strategies and mechanisms to ensure their survival under varying conditions. In some conditions, they balance perturbations by supporting the conditions under which their constitutive processes persists. Altogether these mechanisms are linked to the concepts of 'homeostasis' and 'adaptation', therefore, contribute towards system's viability against perturbations by modifying its own dynamic behaviour. Conclusively, biological regulation enables an organism to control the outcomes of perturbation by regulating its own constitutive dynamics following remarkable alterations in the internal and external conditions (Bich et al. 2016). Thus, the exclusive presence of biological regulation in YADF insects confirms the encounter of these insects with a perturbation (i.e., an enteropathogen in this case).

According to the pathway analysis, 78 assigned EC numbers were identified for the provided unique protein accessions (Supplementary Fig. 1). KEGG pathways (56) were represented by 467 unique protein accessions, including purine metabolism (KO00230: 11 and 4 identified enzymes in control and YADF insects gut, respectively), citrate (TCA cycle) cycle (KO00020: 10 and 6 identified enzymes in control and YADF insects gut, respectively), pyruvate metabolism (KO00240: 9 and 8 identified enzymes in control and YADF insects gut, respectively), glycolysis/gluconeogenesis (KO00010: 9 and 7 identified enzymes in control and YADF insects gut, respectively), starch and sucrose metabolism (KO00500: 8 and 4 identified enzymes in control and YADF insects gut, respectively), and carbon fixation pathways in prokaryotes (KO00720: 7 and 7 identified enzymes in control and YADF insects gut, respectively).

The insect proteins can be differentiated under six categories: proteins involved in (i) melanin synthesis; (ii) stress response and cell redox homeostasis; (iii) cytoskeleton; (iv) iron uptake and storage; (v) anti-pathogenic response; and (vi) metabolism. The proteome comparison between control and YADF insects revealed significantly up-regulated prophenoloxidase

1 (UniProt ID-A0A290U614), prophenoloxidase subunit 2 (UniProt ID-Q2VIY6), serine protease (UniProt ID-O18447), serine protease 5 (UniProt ID-O18436), proteins with serine-type endopeptidase activity (UniProt ID-A0A2W1BP39, UniProt ID-B1NLE3, UniProt ID-O18443, UniProt ID-A0A2W1BGN3, UniProt ID-O18450, UniProt ID-A0A2W1BWI0, and UniProt ID-A0A2W1BVE6), and proteins of serpin family (UniProt ID-A0A2W1BEQ7, UniProt ID-F5B4G8, UniProt ID-A0A2W1BH13, and UniProt ID-A0A290U612); while, significantly down-regulated serine protease inhibitor 6 (UniProt ID-A0A1L5J028) (Table 1).

The proteins related to heat shock response (UniProt ID-C7SIR9, UniProt ID-A0A2H4LI91, UniProt ID-A0A2H4LHM4, UniProt ID-F5BYH9, UniProt ID-A0A2W1BDN4) were significantly up-regulated; whereas, the proteins responsible for cell redox homeostasis (UniProt ID-A0A2W1BQL1, UniProt ID-A0A2W1BSJ9, UniProt ID-A0A2W1BR63, UniProt ID-A0A0A7RB97, UniProt ID-A0A2W1C0K5) and protein folding (UniProt ID-A0A2W1BTU8, UniProt ID-A0A2W1BH57) were significantly down-regulated in YADF insects. The proteins having protective role against oxidative stress, such as catalase (UniProt ID-H9BEW3), glutathione-S-transferase (UniProt ID-A0A0D3M5U4, UniProt ID-A0A2W1BLG9, UniProt ID-A0A291ARU4, UniProt ID-A0A0D3M5T8, UniProt ID-A0A2W1BKA7, and UniProt ID-A0A0D3M5V9), thioredoxin peroxidase (UniProt ID-B2KSE9), and thioredoxin domain containing protein (UniProt ID-A0A2W1C322) were significantly up-regulated in response to the bacterial feeding. Moreover, ferritin (UniProt ID-A0A2W1BW25 and UniProt ID-A0A2W1C098), transferin (UniProt ID-A0A067YAW9), and lipocalin family proteins (UniProt ID-A0A0D3QSH9 and UniProt ID-A0A2W1C146) were significantly up-regulated in YADF insects. The cytoskeleton proteins, including actin (UniProt ID-E2IV58, UniProt ID-A0A221LCD5, UniProt ID-E2IV62) and chitin deacetylase 1 (UniProt ID-D2WPC4) were also found to be up-regulated in the gut of YADF insects. Additionally, proteins with role in cell adhesion (UniProt ID-A0A2W1BP23) and cytoskeleton organization (UniProt ID-A0A2W1BJX1) were significantly down-regulated; while, the protein responsible for actin filament depolymerization (UniProt ID-A0A2W1BIB1) was significantly up-regulated (Table 1). Thus, confirming the affected cytoskeleton of the insect gut in response to *Yersinia* feeding.

Moreover, digestive enzymes such as carboxyester hydrolase of type-B carboxylesterase/lipase family (14) and of lipase family (2), aminopeptidase of peptidase M1 family (6), α-amylase of glycosyl hydrolase family (5), and alkaline phosphatase of alkaline phosphatase family (3) were observed to be significantly up-regulated in YADF insects. Furthermore, metabolic proteins (30), energy metabolism proteins (23), translation-related proteins (23), lipid binding (7), and 5 proteins with lipid transporter activity were found to be differentially expressed in larvae gut after bacterial infection. Proteins including succinate dehydrogenase [ubiquinone] flavoprotein subunit, mitochondrial (UniProt ID-A0A2W1BZK9), succinate dehydrogenase [ubiquinone] iron-sulfur subunit, mitochondrial (UniProt ID-A0A2W1BX81), complex1_30kDa domain-containing protein with NADH dehydrogenase (ubiquinone) activity (UniProt ID-A0A2W1BUD9), uncharacterized protein with NADH dehydrogenase (ubiquinone) activity (UniProt ID-A0A2W1BXT8), and uncharacterized protein with cytochrome-c oxidase activity (UniProt ID-A0A2W1BJ66) were significantly up-regulated in gut of YADF insects (Table 1).

To establish known and predicted protein–protein interactions (PPIs) between the cytoskeleton proteins (15), cell-redox proteins (14), and stress-related heat shock proteins or HSPs (6) from *H. armigera*, an interactome was constructed via $\text{STRING}_{11.0}$ database using *B. mori* as a reference organism. The constructed interactome had 30 nodes and 53 edges with average node degree of 3.53, average local-clustering coefficient of 0.558, and PPI-enrichment p-value of $< 1.0\ e^{-16}$. Moreover, the interactome consisted of three major clusters: (1) between cell-redox proteins (GSTd3, GSTe3, GSTo1, GSTo2, GSTs2, and LOC733095), (2) between cytoskeleton proteins (Kettin, A1, 100101180, BGIBMGA000613-TA, BGIBMGA003515-TA, BGIBMGA014226-TA, and BGIBMGA001730-TA), and 3) between stress-related HSPs and cell-redox proteins. The cell redox proteins GSTs2 and BGIBMGA002818-TA were found to connect the clusters (1) and (3). Likewise, the cytoskeleton proteins A1 and 100101180 connected the clusters (2) and (3) by interacting with stress-related proteins HSP70 and 14-3-3zeta,

Table 1 List of up-regulated and down-regulated proteins in YADF insects

Accession number	Name	MW (kDa)	calc. pI	# Peptides	Coverage (%)	Expression
A0A2W1BUD9	Uncharacterized protein	30.4	6.71	10	42	1.322
A0A2W1BZK9	Succinate dehydrogenase [ubiquinone] flavoprotein subunit, mitochondrial	71.2	6.99	7	17	1.044
A0A2W1C098	Ferritin	23.7	5.27	7	33	0.948
A0A067YAW9	Transferin	82.9	6.14	11	27	0.926
A0A2W1BGN3	Uncharacterized protein (Fragment)	90.6	6.32	5	6	0.848
A0A0D3M5V9	Glutathione S-transferase GSTD3	24.8	6.65	4	28	0.848
A0A291ARU4	Glutathione S-transferase	24.4	5.44	12	71	0.833
A0A2W1BP39	Uncharacterized protein	26.9	8.51	4	33	0.807
A0A2W1BEQ7	Uncharacterized protein	51	5.29	10	30	0.778
O18436	Serine protease 5	26.9	8.69	4	33	0.737
B1NLE3	Protease	35.9	4.42	5	28	0.710
A0A221LCD5	Actin (Fragment)	14.4	5.49	11	95	0.704
E2IV62	Actin	41.8	5.48	31	85	0.605
A0A0D3M5T8	Glutathione S-transferase GSTS4	16.5	5.38	12	79	0.585
A0A2W1BW25	Ferritin	13.2	5.74	4	55	0.585
D2WPC4	Chitin deacetylase 1	61.7	5.21	6	18	0.585
O18447	Serine protease	26.9	9.06	7	46	0.485
A0A2W1BIB1	Uncharacterized protein	17	6.57	9	55	0.469
E2IV58	Actin	41.8	5.31	37	78	0.435
A0A2W1BKA7	Uncharacterized protein (Fragment)	32.1	6.62	7	45	0.433
A0A0D3M5U4	Glutathione S-transferase GSTS1	24.7	6.61	17	72	0.392
A0A2W1BX81	Succinate dehydrogenase [ubiquinone] iron-sulfur subunit, mitochondrial	31.9	8.27	8	26	0.392
A0A2W1BJ66	Uncharacterized protein	17	5.43	9	56	0.363
A0A2H4LHM4	Heat shock protein 60	61	5.72	35	70	0.359
B2KSE9	Thioredoxin peroxidase	22	6.34	14	75	0.333
H9BEW3	Catalase	56.7	7.84	23	47	0.322
C7SIR9	Heat shock protein 70	71.6	5.38	39	71	0.293
A0A2H4LI91	Heat shock cognate protein 70	71.6	5.47	42	73	0.269
F5BYH9	Heat shock protein	73	5.3	33	54	0.268
A0A290U612	Serpin-9	45.3	5.12	11	38	0.263
A0A2W1BDN4	Uncharacterized protein	74.9	6.21	27	53	0.233
O18450	Chymotrypsin-like protease	30.8	8.51	13	64	0.231
A0A2W1BWI0	Uncharacterized protein	38.7	4.4	6	28	0.206
A0A0D3QSH9	Polycalin	101.6	4.73	10	23	0.198
A0A2W1BXT8	Uncharacterized protein	79.7	6.96	20	36	0.189
A0A2W1BH13	Uncharacterized protein	44.8	5.16	20	52	0.170
F5B4G8	Serpin	43.5	5.17	15	50	0.132
Q2VIY6	Prophenoloxidase subunit 2	80.1	6.18	26	55	0.130
A0A290U614	Prophenoloxidase 1	78.6	6.74	28	55	0.121
O18443	Chymotrypsin-like protease (Fragment)	29.2	8.29	4	20	0.100
A0A2W1BVE6	Uncharacterized protein	92.7	5.05	8	12	0.100
A0A2W1C322	Uncharacterized protein	47.2	6.19	7	29	0.100
A0A2W1C146	Uncharacterized protein	272.9	4.74	19	15	0.087

Table 1 continued

Accession number	Name	MW (kDa)	calc. pI	# Peptides	Coverage (%)	Expression
A0A2W1BLG9	Uncharacterized protein	29	7.02	9	48	0.082
A0A2W1C0K5	Dihydrolipoyl dehydrogenase	55.2	8.73	11	32	− 0.032
A0A2W1BTU8	Peptidyl-prolyl cis–trans isomerase	20.9	8.88	7	43	− 0.093
A0A1L5J028	Serine protease inhibitor 6	46.6	5.87	11	31	− 0.290
A0A2W1BQL1	Uncharacterized protein	46.7	5.38	9	29	− 0.290
A0A2W1BH57	Uncharacterized protein	82.6	5.07	16	26	− 0.348
A0A2W1BR63	Uncharacterized protein	235.1	4.32	13	10	− 0.415
A0A2W1BJX1	Adenylyl cyclase-associated protein	82.9	5.9	9	19	− 0.415
A0A2W1BSJ9	Uncharacterized protein	50.6	4.74	36	72	− 0.439
A0A2W1BP23	Uncharacterized protein	451.7	5.86	14	6	− 0.515
A0A0A7RB97	Thioredoxin reductase	57	7.65	7	28	− 0.585

respectively. Further, the cytoskeleton protein BGIBMGA000613-TA of cluster (2) was found to interact with the cell redox protein BGIBMGA008023-TA of cluster (3) (Fig. 3). The protein interactions between up-regulated 14-3-3zeta with up-regulated 100101180 (actin filament depolymerization) and down-regulated BGIBMGA008023-TA with down-regulated BGIBMGA000613-TA (motor activity) further strengthened the hypothesis of stress-induced damage of *Helicoverpa* gut epithelium in response to enteropathogen infection (Fig. 3; Table 2).

Effect of *Y. enterocolitica* infection on *H. armigera* larvae gut

The larvae of two days old (first-instar) neonates of *H. armigera* were orally challenged with virulent strain, i.e., *Y. enterocolitica* strain 8081 (1B/O:8) in the artificial diet, till fourth-instar. The control insects

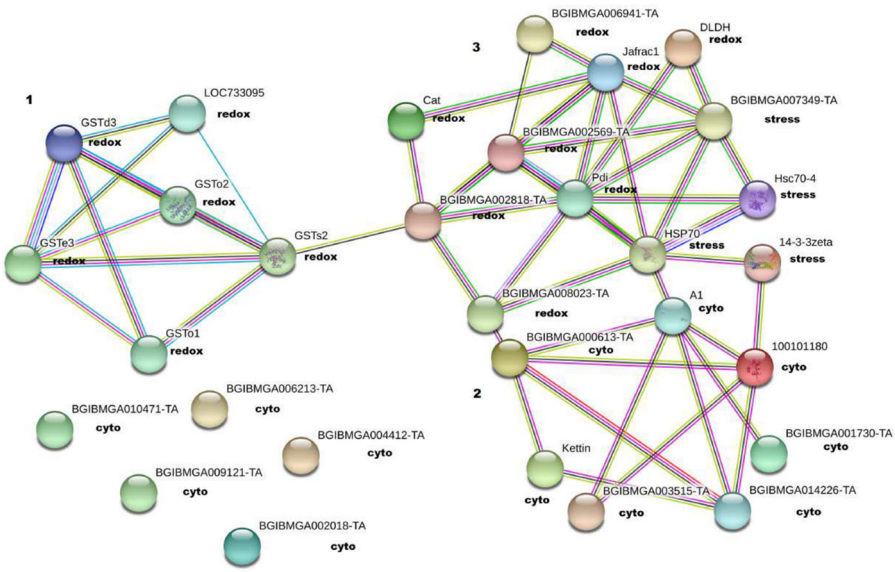

Fig. 3 Protein interaction network of differentially expressed (of interest) proteins generated with STRING (ver. 11.0). Nodes represent proteins and edges represent protein–protein interactions (PPIs). Empty nodes represent proteins of unknown 3-D structure and filled nodes represent known or predicted 3-D structure. The 'cyto', 'stress' and 'redox' represents cytoskeleton proteins, stress-related HSPs, and cell-redox proteins, respectively

Table 2 List of proteins used for protein–protein interactions (PPIs) study

S. No	Accession no	UniProt name	STRING name	Function	Family
Cytoskeleton proteins					
1	**E2IV58**	**Actin**	**A1**	**–**	**Actin family**
2	**A0A2W1BJV8**	**Uncharacterized protein**	**A1**	**ATP binding**	**Actin family**
3	**A0A221LCD5**	**Actin**	**A1**	**–**	**Actin family**
4	A0A2W1BP23	Uncharacterized protein	BGIBMGA002018-TA	Cell adhesion	–
5	A0A2W1BJX1	Adenylyl cyclase-associated protein	BGIBMGA003515-TA	Actin binding, cell morphogenesis, cytoskeleton organization	CAP family
6	**D2WPC4**	**Chitin deacetylase 1**	**BGIBMGA006213-TA**	**Chitin binding, hydrolase activity, acting on carbon–nitrogen (but not peptide) bonds, carbohydrate metabolic process, chitin metabolic process**	–
7	A0A2W1BGZ7	Uncharacterized protein	BGIBMGA004412-TA	Actin binding	–
8	**A0A2W1BNN9**	**Uncharacterized protein**	**BGIBMGA014226-TA**	**Actin filament binding, ATP binding, motor activity**	**Myosin kinase ATPase superfamily, Mysoin family**
9	A0A2W1BVZ9	Uncharacterized protein	BGIBMGA000613-TA	Motor activity	–
10	**E2IV62**	**Actin**	**A1**	**Actin binding**	**Actin family**
11	A0A2W1BHR2	Uncharacterized protein	BGIBMGA001730-TA	Actin filament binding	–
12	A0A2W1BED4	Uncharacterized protein	BGIBMGA010471-TA	Actin binding	–
13	A0A2W1C0G2	Uncharacterized protein	BGIBMGA009121-TA	Actin binding, structural molecule activity	–
14	**A0A2W1BIB1**	**Uncharacterized protein**	**100101180**	**Actin binding, actin filament depolymerisation**	**Actin-binding proteins ADF family**
15	A7Y0T5	Kettin1 protein	Kettin	–	–
Stress-related heat shock proteins (HSPs)					
16	**C7SIR9**	**Heat shock protein 70**	**Hsc70-4**	**ATP binding (stress response)**	**Heat shock protein 70 family**
17	**A0A2H4LI91**	**Heat shock cognate protein 70**	**Hsc70-4**	**ATP binding (stress response)**	**Heat shock protein 70 family**

Table 2 continued

S. No	Accession no	UniProt name	STRING name	Function	Family
18	**A0A2H4LHM4**	**Heat shock protein 60**	**BGIBMGA007349-TA**	**ATP binding, protein refolding**	**Chaperonin (HSP60) family**
19	**F5BYH9**	**Heat shock protein**	**HSP70**	**ATP binding (stress response)**	**Heat shock protein 70 family**
20	**A0A2W1BDN4**	**Uncharacterized protein**	**HSP70**	**ATP binding, unfolded protein binding, protein folding**	**Heat shock protein 70 family**
21	**A0A2W1BFL3**	**Uncharacterized protein**	**14-3-3zeta**	**Protein domain specific binding**	**14–3-3 family**
Cell-redox proteins					
22	A0A2W1BSJ9	Uncharacterized protein	Pdi	Isomerase activity, cell redox homeostasis	–
23	A0A0A7RB97	Thioredoxin reductase	BGIBMGA002818-TA	Electron transfer activity, flavin adenine dinucleotide binding, thioredoxin-disulfide reductase activity, cell redox homeostasis	Class-I pyridine nucleotide-disulfide oxidoreductase family
24	A0A2W1C0K5	Protein Dihydrolipoyl dehydrogenase	DLDH	Dihydrolipoyl dehydrogenase activity, electron transfer activity, flavin adenine dinucleotide binding, cell redox homeostasis	Class-I pyridine nucleotide-disulfide oxidoreductase family
25	**B2KSE9**	**Thioredoxin peroxidase**	**Jafrac1**	**Peroxidase activity, peroxiredoxin activity, cell redox homeostasis**	–
26	A0A2W1BQL1	Uncharacterized protein	BGIBMGA002569-TA	Isomerase activity, cell redox homeostasis	Protein disulfide isomerase family
27	A0A2W1BR63	Uncharacterized protein	BGIBMGA008023-TA	Cell redox homeostasis	–
28	**A0A2W1C322**	**Uncharacterized protein**	**BGIBMGA006941-TA**	**Cell redox homeostasis**	–
29	**H9BEW3**	**Catalase**	**Cat**	**Catalase activity, heme binding, metal ion binding, hydrogen peroxide catabolic process, response to oxidative stress**	**Catalase family**
30	**A0A2W1BLG9**	**Uncharacterized protein**	**GSTo1**	**Glutathione transferase activity**	**GST superfamily**
31	A0A0F6Q4I6	S-(hydroxymethyl)glutathione dehydrogenase	LOC733095	S-(hydroxymethyl)glutathione dehydrogenase activity, zinc ion binding, ethanol oxidation	Zinc-containing alcohol dehydrogenase family, Class-III subfamily
32	**A0A291ARU4**	**Glutathione S-transferase**	**GSTd3**	**Transferase activity**	–
33	**A0A2W1BKA7**	**Uncharacterized protein**	**GSTo2**	**Glutathione transferase activity**	–

Table 2 continued

S. No	Accession no	UniProt name	STRING name	Function	Family
34	**A0A0D3M5T8**	**Glutathione S-transferase GSTS4**	**GSTs2**	**Transferase activity**	–
35	**A0A0D3M5V9**	**Glutathione S-transferase GSTD3**	**GSTe3**	**Transferase activity**	–

Bold represents the up-regulated proteins

were fed with the artificial diet. The larvae survival was observed over time after feeding of the bacterial suspension such that no mortality was reported in either group. However, the bacterial infection noticeably affected the feeding, development, and behavior of the infected larvae. Post infection, the larvae become morbid and the feeding was also reduced. The initial average body weight of the larva was 0.22 ± 0.014. The reported body weight of control and YADF insects (fourth-instar) were 375.63 ± 32.59 mg and 253.87 ± 66.78 mg, respectively (Fig. 4A, Supplementary Table 4). The data was statistically analyzed which showed significant reduction in the average body weight of ten days old (fourth-instar) YADF insects (Fig. 4A), where A, B, and C represents 10^{-1}, 10^{-2}, and 10^{-3} dilution, respectively.

Biochemical and spectroscopic studies

The gut of ten days old (fourth-instar) larvae were dissected aseptically and homogenized for further analysis. The GSH level was found to slightly decreased (0.41 fold); whereas, the CAT activity increased by 2.52 fold in YADF insects gut. Higher (2.83 fold) MDA level in YADF insects gut showed enhanced LPO in comparison to the control larval gut (Table 3).

Fourier-transform infra-red (FTIR) spectroscopy provides a fast and label-free tool to study the molecular composition of a sample without perturbing it. It depends on quantitatively measuring the IR active-vibrational modes of the molecular bonds with an electric dipole moment, which change by the atomic displacement. For biological samples, the significant spectral regions quantified are the finger-print region (450 cm^{-1}, 600 cm^{-1}) and amide I/II region (700 cm^{-1}, 1500 cm^{-1}). The higher wavenumber region, i.e., 2550–3500 cm^{-1} corresponds to stretching vibrations like C–H, S–H, O–H and N–H; whereas, the lower-wavenumber region is associated with bending and C-skeleton finger-print vibrations. Together, these regions provide a finger-print of structure of the specimens (Baker et al. 2014). The FTIR spectroscopic analysis showed a variation with the absence of peaks (in YADF insect) at 3258 cm^{-1}, 2838 cm^{-1}, and 1745 cm^{-1}, indicating N–H stretching, C–H stretching, and C=O stretching, respectively. A shift of peak from 1376 cm^{-1} (in control) to 1397 cm^{-1} (in YADF insect) was due to C-H bending

(Fig. 4B, Supplementary Table 5). Additional peaks at 998 cm^{-1} for C–H bending, and 1078 cm^{-1} for C–C multiple bond stretching was observed in control larval gut. Various additional peaks from 500 to 900 cm^{-1} were observed in gut of control larvae. Altogether, these variations suggested the change in biological macromolecules including proteins, nucleic acids, lipids, and carbohydrates.

Imaging studies of YADF insects gut

The scanning electron micrographs of the surface of control and YADF insects midgut epithelium appeared with densely packed microvilli. However, cell loosening and widening was observed in YADF insects midgut epithelium (Fig. 5A, B). This is in concurrence with down-regulated proteins with role in cell adhesion and cytoskeleton organization. Histopathological observations do not show any significant difference between control and YADF insects midgut epithelium besides slight erosion or cell loosening (Fig. 5C, D).

Discussion and conclusion

Upon oral challenge with *Y. enterocolitica* strain 8081, no mortality but significant reduction in average body weight was observed in *H. armigera* larvae. This was supported by an earlier report in *G. mellonella-Y. enterocolitica* strain 8081 infection model (Alenizi et al. 2016). As reported earlier, 57 colony forming unit (CFU) of *Y. enterocolitica* strain 8081 killed almost all larvae of *G. mellonella* at 15 °C, but 40 CFU killed only 4% larvae at 30 °C; thus, showing the temperature-dependent toxicity of this pathogen in *G. mellonella* infection model (Springer et al. 2018). Similarly, another study on developing *G. mellonella* larvae as an in vivo model system for evaluating the virulence of *Shigella* showed time-dependent larval death accompanied by melanization (Barnoy et al. 2017). According to a previous work, the oral feeding of *Y. enterocolitica* (WA-314 pYVO8 +) to 6–8 weeks old female C57BL/6 mice caused a significant reduction in mean weight, two days post infection (Hering et al. 2016).

On performing label-free proteomics, putative hemolysin and secretory systems were emerged as the main *Yersinia*-identified proteins along with proteins for sensing, signaling and regulation. Previous study involving genomic comparison approach identified 329 genes that were present in highly-insecticidal strains (*Yersinia intermedia* and *Yersinia frederiksenii*) and absent in weakly-insecticidal strain (*Yersinia enterocolitica* strain W22703). Similar to the proteins identified in the present study, the products of previously-identified genes belong to the following categories: lipoproteins and other membrane proteins, metabolism, resistance toward toxic substances, sensing, signaling and regulation, transport and secretion, putative adhesins, toxins, hemolysins and secretory systems, stress response, iron uptake and storage (Springer et al. 2018). The gram-negative entomopathogenic bacteria have developed various strategies including specialized secretion systems to interact

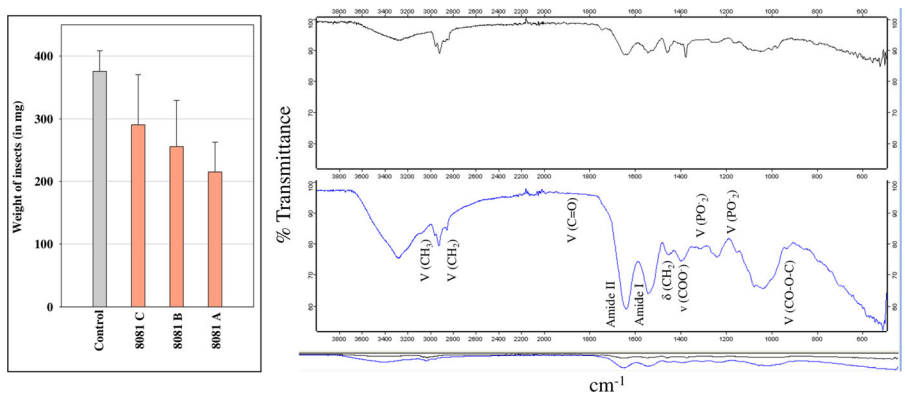

Fig. 4 **A** Reduction in body weight of *H. armigera* larvae after treatment with different concentration of *Y. enterocolitica* strain 8081. 8081 (A, B, and C) represents 10^{-1}, 10^{-2}, and 10^{-3} dilution, respectively and * represents differences between control (artificial diet-fed) insects and YADF insects (unpaired student's *t*-test $p < 0.05$) **B** Biological FTIR-spectrum showing biomolecular peak assignments for control (in blue) and YADF insects [fourth-instar (in black)] gut samples

Table 3 Catalase (CAT), gluthathione (GSH) and malondialdehyde (MDA) levels in the gut homogenates of control and YADF insects

Parameter and unit	Control insects	YADF insects
CAT (nmol of H_2O_2 decomposed/min/mg protein)	1.757 ± 0.155	4.425 ± 0.561
GSH (μg glutathione/mg protein)	0.360 ± 0.0166	0.151 ± 0.0018
MDA (nmol MDA/mg protein)	12.490 ± 1.177	35.455 ± 5.215

with the insects to kill them. The secretion systems transport several proteins from bacterial cytosol to surface, into the environment or directly into the host cells, where they have role in stimulating the virulence (McQuade and Stock 2018). From an earlier work, *Y. frederiksenii* and *Y. intermedia* were shown to carry a T6SS, which along with other functions, adds to the virulence (Springer et al. 2018). Additionally, the pathogenicity of *Y. enterocolitica* depends on T3SS. The secretion system facilitates the injection of virulence factors or Yops into the cytosol of the host cells. Yops modulates the cytoskeleton, thereby inhibiting the phagocytosis and inducing the cell death (Rakin et al. 2015). Inside insect hosts, *Y. enterocolitica* are confronted by changing and hostile surrounding conditions, which they have to sense and adapt to for their persistence. Interestingly, bacteria have evolved the two-component systems to sense and to react rapidly to the changing surrounding conditions. They are involved in metabolite utilization, regulation of symbiosis or virulence, and in adaptation to many stress factors. Additionally, in an earlier work,

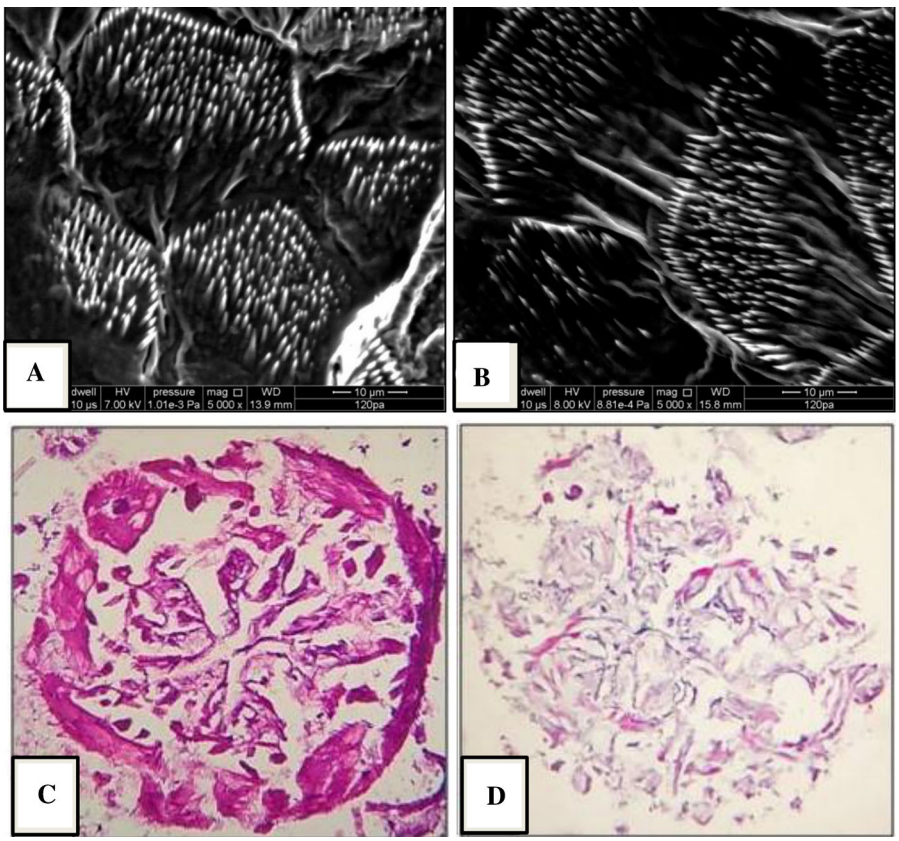

Fig. 5 Scanning electron microscopy (SEM, X5000) of midgut of *H. armigera* larvae: **A** control **B** treated with *Y. enterocolitica* strain 8081.Hematoxylin–eosin (H-E) staining (X40) of midgut of *H. armigera* larvae: **C** control **D** treated with *Y. enterocolitica* strain 8081

five virulence-associated (*vag*) genes including *vag*H, a methyltransferase were reported to be linked to virulence in mice as shown by infection with *Yersinia*. Other methyltransferases, *vag*B and *vag*E were found to be not essential but contained within operons involved in virulence (Garbom et al. 2004). Another report suggested that the ABC transporter genes *irp6* and *irp7* are required for mouse virulence in *Y. enterocolitica* O:8 (Brem et al. 2001). Further, *nudA* gene encoding a Nudix hydrolase is reported to be a virulence factor and important for resisting stress in *Legionella pneumophila* (Edelstein et al. 2005). The product of YPTB0333 gene encoding a transcriptional regulator from LysR family is found to control genes encoding Yfe iron-uptake system and polymyxin B resistance. Such that, using a mouse model of oral infection, it was shown that YPTB0333 is required for the colonization of Peyer's patches and mesenteric lymph nodes by *Y. pseudotuberculosis* (Arafah et al. 2009). Further, penicillin-binding protein 1B [*Escherichia coli* O44:H18 (strain 042/EAEC)], p-hydroxybenzoic acid efflux pump subunit AaeB [*E. coli* O26:H11 (strain 11368/EHEC)], and UDP-4-amino-4-deoxy-L-arabinose–oxoglutarate aminotransferase [*E. coli* O26:H11 (strain 11368/EHEC)] was found to be associated with antibiotic resistance (Manrique et al. 2011). Thus, the proteomic occurrence of the above mentioned pathogenic proteins in YADF insects gut supports the induced infection.

In insect, proteomics suggested increased melanization, i.e., insect innate immune response to infection and damage to host, which can be defined as the synthesis and deposition of melanin to encapsulate the pathogens at the injury site, accompanied by coagulation and opsonization. It is similar to the formation of abscess in mammalian infection (Tsai et al. 2016). Melanin synthesis is catalyzed by enzyme phenoloxidase (PO) that is produced as an inactive prophenoloxidase (PPO). Insect PPO is a crucial innate immunity protein due to its involvement in humoral and cellular defense. During a microbial infection, PPO cascade is activated by serine proteases that cleave PPO to PO. The activated PO transforms phenolic substrates to quinones, which polymerize to form melanin around wounds and invading pathogens. PO also produces reactive oxygen species (ROS), cytotoxic quinines, and reactive nitrogen that cause tissue toxicity; and therefore, its activation is tightly regulated by protease inhibitors. In a previous proteomic study on *B. bassiana*-infected silkworm, the expression levels of serine protease (NP_001036826) was up-regulated and of serine protease inhibitors, i.e., chymotrypsin inhibitor CI-8A (AAK52495), chymotrypsin inhibitor fb (AAK52496), fungal protease inhibitor F-like (XP_004924401), and serine protease inhibitor 7 precursor (NP_001139701) were down-regulated after *B. bassiana* infection. Thus, suggesting their role in melanization and defense against the fungal pathogens (Lü et al. 2019). Another study on baculovirus-infected *H. armigera*, reported that the infection induced serpin-5 and serpin-9 inhibits clip-domain serine proteases (cSPs), which resulted in reduced PO activity, to suppress the host melanization for the pathogen survival (Yuan et al. 2017).

The proteomics study further confirmed the affected metabolism of the insect gut in response to *Yersinia* feeding. Previous proteomic work on *Wolbachia* strain *w*Str-infected *Aedes albopictus* C/*w*Str1 cells, reported elevated energy metabolism proteins in infected cells. It may supplement the amino acids as well as the precursors for lipid and nucleic acid biosynthesis, which cannot be synthesized by the bacteria. Further, up-regulated superoxide dismutases (SODs), thioredoxins (Trxs), and peroxidases (PODs) indicated a response to oxidative stress in the infected cells. Collectively, altered metabolic signaling, protein degradation pathways and autophagy; with elevated TCA cycle and amino acid metabolism proteins suggests that the bacterial replication within the host-derived vacuoles escapes xenophagy, and sequesters the host-derived amino acids (Baldridge et al. 2017). Another proteomic study, to evaluate the alterations in *C. elegans* during *Pseudomonas aeruginosa* PAO1 infection, suggested the changed expression of TCA cycle proteins and oxidative phosphorylation machinery. Thereby, inducing the oxidative stress impaired protein homoeostasis mechanisms (Mir and Balamurugan 2019). Moreover, in the present study, ferritin, transferrin, and proteins with protective role against oxidative stress and heat shock response were significantly up-regulated; whereas, the proteins responsible for cell redox homeostasis were significantly down-regulated in response to the bacterial feeding. In this regard, a previous study on silkworm showed high expression of *B. mori* thioredoxin peroxidase (BmTPx) enzyme in response to baculovirus infection, suggesting the protective role of BmTPx against

oxidative stress (Lee et al. 2005). Further, insect thioredoxin (Trx) is a thiol-dependent redox system, which regulates the responses generated by oxidative stress, with a prominent role in maintaining the cell redox homeostasis (Nappi and Christensen 2005). Ferritin and transferrin have important roles in iron storage and transport, respectively. Ferritins store excess iron and play a crucial role in iron homeostasis and management of the oxidative stress response in the invertebrates. Crustacean ferritins are implicated in innate immunity against the pathogens and resistance to various stresses (Tang et al. 2019). As known previously, specific innate immune responses limit iron availability to microbes during infection by decreasing the plasma iron concentrations within hours of infection. This response has been documented in mammals, including humans and other vertebrates (Ganz 2018). In a recent work, novel red fluorescent protein (RFP) was purified from the midgut of silkworm, whose N-terminal sequencing predicted *chbp* gene of lipocalin gene family with anti-pathogenic activities (Manjunatha et al. 2018). In corroboration to proteomics data, the biochemical assays depicting higher MDA level in YADF insects gut suggested enhanced LPO in comparison to the control larval gut. This causes loss of membrane integrity. Further, enhanced LPO and altered levels of antioxidant enzymes results in oxidative stress; thus, producing deleterious effects on the growth and development of *H. armigera* (Ahlawat et al. 2020). As reported previously, haemocytes produce free radicals to battle infections. Increased production of free radicals were observed between control group and *Streptococcus pneumoniae* (strain TIGR4 and D39)-infected larvae (Cools et al. 2019). Another study on *Tenebrio molitor* larvae infected with *Heterorhabditis beicherriana* suggested increased activities of superoxide dismutase (SOD), peroxidase (POD), catalase (CAT), and tyrosinase (TYR). Other detoxifying enzymes, like glutathione S-transferase (GST), carboxylesterase (CarE), and acetylcholinesterase (AChE) were also increased at lower infection rates suggesting that the host anti-oxidative response and detoxifying enzymes played an important role in the defensive reaction to infection (Li et al. 2016). However, ROS are also generated during respiration by respiratory complexes of mitochondrial electron-transport chain. Released ROS induces oxidative stress that caused increased expression of the stress response and cell redox homeostasis proteins. Further, increased activity of antioxidant enzymes was reported in entomopathogenic nematodes-infected *G. mellonella* larvae that suggests increased oxidative stress and anti-oxidative responses in response to the infection (Wu and Liu 2012).

Lastly, proteomics confirmed the affected cytoskeleton of the insect gut in response to *Yersinia* infection, as suggested by the histopathological and SEM analysis. Earlier report, also suggested depolymerization of actin stress fibres in eukaryotes after T3SS-injected YopE, an essential virulence determinant of *Yersinia pseudotuberculosis* (Von Pawel-Rammingen et al. 2000). Another study, reported reduced peritrophic membrane permeability (due to down-regulated midgut-specific chitin deacetylase-like protein) as a possible mechanism used by *H. armigera* to reduce the susceptibility to baculovirus (Jakubowska et al. 2010). Further, variations in IR peaks suggested change in biological macromolecules, which might be mediated by the generated ROS that impairs cell activities, such as gene expression and membrane function. In a previous work, damaged DNA in haemocytes of *G. mellonella* larvae was observed after *Actinobacillus pleuropneumoniae* infection. *A. pleuropneumoniae* cytotoxic factors cause damage to haemocyte DNA, thereby, killing and reducing the number of these cells in the larva. This effect is one of the mechanisms used by microbial cells to evade the host immune system (Pereira et al. 2015). Another study on *Y. enterocolitica* (WA-314 pYVO8 +) infected mice model system showed that the pathogen invade the colon mucosa by altering the tight junction (TJ) protein expression and architecture (Hering et al. 2016). Most of digestive and absorptive functions occur in the midgut of insect, such that any damage in midgut affects its growth and development, which eventually reduces the body weight (Marzban et al. 2013).

Finally, PPIs among proteins was studied via $STRING_{11.0}$ software that revealed three interaction clusters generated: one between cell-redox proteins, another between cytoskeleton proteins, and third between stress-related HSPs and cell-redox proteins. Recent study based on interactome analyses (via $STRING_{10.5}$) of *C. elegans* (host)—*Salmonella enterica* serovar Typhi (interacting pathogen) proteins demonstrated HSP-90 as a central player which coordinated other identified proteins and had role

during pathogenic defense. Further, it was revealed to be up-regulated during (24 and 48 h) infection. This suggested that HSP-90 is required for regulatory events during infection in the host (Balasubramaniam et al. 2019). Another recent label-free proteomic work on LPS-537 treated sea urchin *Paracentrotus lividus* showed that LPS-treatment can modulate several processes like cytoskeleton re-organization, stress by induction of HSPs, and energetic homeostasis. The interactomes were also constructed by the early workers. It showed four clusters, mainly composed of cytoskeleton & cytoskeleton-related factors, RAS superfamily GTPase members, heat shock proteins (HSPs), and histones. The results confirmed that the cytoskeleton re-organization is a last process that is restored after the treatment (Inguglia et al. 2020).

Hence, pathogenicity is an outcome of both host and microbial factors—a concept described as the "damage-response framework". Insect consists of cellular and humoral innate immune responses, where cellular component is composed of hemocytes and humoral defense includes soluble immune factors of hemolymph. The most significant immune response in insects is melanin synthesis, which occurs in response to the microbial invasion (Krachler et al. 2021). The key component of *Yersinia*–host cell interaction is its linkage with neutrophils during tissue infection. Neutrophils as crucial cells of innate immune system, it sense and kill pathogens by releasing signaling molecules and via degranulation, formation of neutrophil extracellular traps (NETs), generation of ROS, and phagocytosis, respectively. After infection with *Yersinia*, neutrophils migrate rapidly (with a delay in comparison to the recruitment by a yop mutant) to the Peyer's patches and eventually encase the bacterial colonies such that they become the most adjacent cell-type to *Yersinia*. The delay demonstrates that a very early Yop injection into tissue cells modulates cytokine and chemokine release and retards the neutrophil recruitment. For instance, the replication of *Y. pestis* in draining lymph nodes induces very little host cytokine response that is inhibited by T3SS along with the other components of virulence plasmid. But later, neutrophils with other phagocytes are recruited to infected lymph nodes and IL-17 is produced. Similarly, immune responses to *Y. enterocolitica* and *Y. pseudotuberculosis* in Peyer's patches are marked by neutrophil influx and TH_{17}/TH_1 response (Davis 2018). In return, neutrophils are successively injected with Yops by *Yersinia* during infection as *Yersinia* has an ability to combat neutrophil invasion within the tissues. The T3SS effector proteins manipulate the host defense system to allow pathogen survival by inhibiting phagocytosis and inflammatory pathways that withstand T3SS innate immune recognition (Schubert et al. 2020).

Further, the existing evidences also suggest the ability of *Yersinia* to withstand ROS, as its growth is not influenced by the presence or absence of host-derived ROS (Davis 2018). Thus, pathogenicity of *Yersinia* in vertebrates has been shown to be affected by both bacteria-driven processes and host response-driven damage (Krachler et al. 2021). The above accounted host (mammals including humans) response to *Yersinia* is also observed in present study in *H. armigera* host. *Yersinia* infection in both hosts (mammals and *H. armigera*) induces the expression of proteins related to innate immune response, oxidative stress, and cytoskeleton. Further, similar *Yersinia* pathogenic proteins such as T3SS and others were also observed in both hosts (mammals and *H. armigera*) (Table 4). Thus, based on the theory of "damage-response framework" it can be concluded that *Yersinia* undoubtedly establishes the infection condition inside the insect midgut that truly mimics mammals gut interactions.

In conclusion, the experimental findings suggest that *H. armigera* larva can be considered as a potential in vivo model for studying the enteropathogenic infection by *Y. enterocolitica* strain 8081. Label-free proteomic analysis via an Orbitrap nano-LC–MS/MS helped to know the interaction of the enteropathogen with the insect host. In present study, the active infection by *Y. enterocolitica* strain 8081 in this model system led to its survival and growth, which is dependent upon the production of intact virulence factors like T3SS, T6SS, and hemolysins. In response, *H. armigera* responded to bacterial infection by significant induction of melanization, iron uptake proteins, and anti-pathogenic response proteins of the lipocalin family to limit the infection. In brief, *Y. enterocolitica* strain 8081 infection induces innate immune response in the insect gut that synthesizes melanin around the invading pathogen. In a cascading effect, ROS is generated that caused damage in YADF insects gut (Fig. 6). Thus, *H. armigera* can be used as an alternate, rapid, efficient, ethically acceptable, and cost-effective insect model system to study the

Table 4 Pathogenic and host-response proteins common in both *Yersinia* infected mammals and *H. armigera* model (present study)

Pathogenic proteins			Host-response proteins		
Virulence			Innate immune response		
Protein		UniProt ID	Protein		UniProt ID
Secretory system	T3SS	A0A2K7ZFA6	Prophenoloxidase 1		A0A290U614
	T6SS	A0A0B6FGX6	Prophenoloxidase subunit 2		Q2VIY6
Two-component system	Response regulator	A0A0B6FI68	Serine protease		O18447
	Phosphotransferase RcsD	A0A0T9ST75	Serine protease 5		O18436
	Sensor histidine kinase RcsC	A0A0H5H628	Serine protease inhibitor 6		A0A1L5J028
	Histidine kinase	A0A2J9SBL6	Serpin		F5B4G8
Methyltransferases		A0A0T7NWH8	Serpin-9		A0A290U612
		A0A2K7ZKH5			
ABC transporter		A0A0U1HE06			
Nudix hydrolase		A0A2J9SIN6			
Transcriptional regulator from LysR family		A0A2J9S9G4			
Hemolysin		A0A0H3NJZ6			
Antibiotic resistance			Oxidative stress-induced tissue destruction		
Penicillin-binding protein 1B		A0A0H3NY99	Ferritin		A0A2W1C098, A0A2W1BW25
p-hydroxybenzoic acid efflux pump subunit AaeB		A1JRH8	Antioxidants	Glutathione S-transferase	A0A291ARU4
UDP-4-amino-4-deoxy-L-arabinose–oxoglutarate aminotransferase		A0A0T9SLB5		Glutathione S-transferase GSTS1	A0A0D3M5U4
				Glutathione S-transferase GSTD3	A0A0D3M5V9
				Glutathione S-transferase GSTS4	A0A0D3M5T8
				Catalase	H9BEW3
				Thioredoxin peroxidase	B2KSE9
				Thioredoxin reductase	A0A0A7RB97
			HSPs	Heat shock protein	F5BYH9
				Heat shock protein 60	A0A2H4LHM4
				Heat shock protein 70	C7SIR9
				Heat shock cognate protein 70	A0A2H4LI91
			Cytoskeleton		
			Actin		E2IV58, E2IV62
			Actin (Fragment)		A0A221LCD5
			Chitin deacetylase 1		D2WPC4
			Uncharacterized protein (actin filament depolymerization)		A0A2W1BIB1
			Uncharacterized protein (cell adhesion)		A0A2W1BP23
			Adenylyl cyclase-associated protein (cell organization)		A0A2W1BJX1

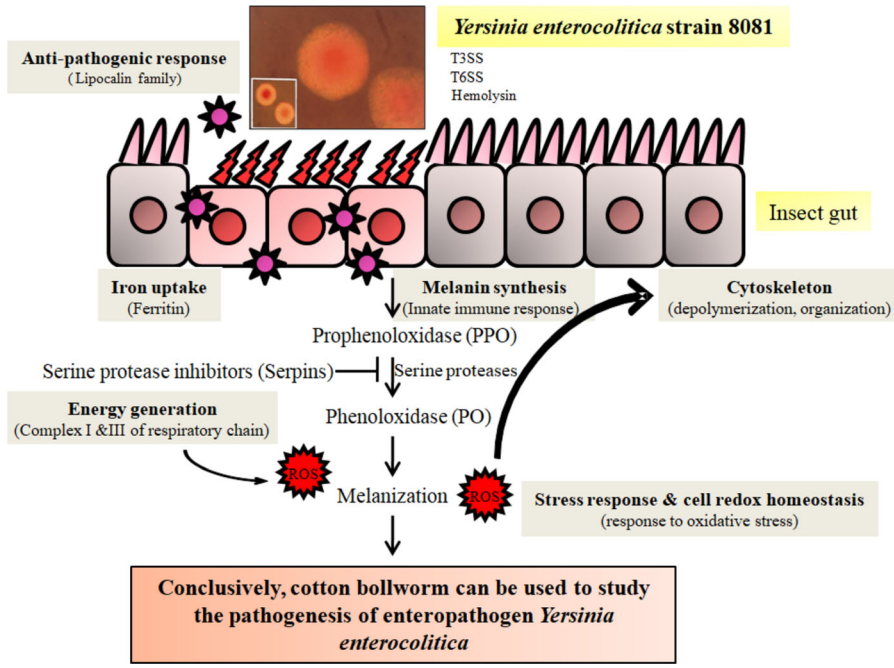

Fig. 6 Summary of *Y. enterocolitica* infection induced protein alterations in *H. armigera* model system

pathogenesis of enteropathogens, including *Y. enterocolitica*.

Acknowledgements The authors thank Prof. Deepak Pental, Centre for Genetic Manipulation of Crop Plants (CGMCP), University of Delhi South Campus, New Delhi, India for the insect trial facility. The authors would also like to acknowledge the anonymous reviewers for the meticulous editing.

Author contributions All authors read and approved the manuscript.

Funding This research did not receive any specific grant from funding agencies in the public, commercial, or not-for-profit sectors.

Data availability The raw data supporting the conclusions of this manuscript will be made available by the authors, without undue reservation, to any qualified researcher. The mass spectrometry proteomics data have been deposited to the ProteomeXchange consortium via the proteomics identification database (PRIDE; https://www.ebi.ac.uk/pride/) partner repository with the dataset identifier PXD021304.

Declarations

Conflict of interest The authors declare that they have no known competing financial interests or personal relationships that could have appeared to influence the work reported in this paper.

Ethical approval *H. armigera* has not been notified under any act or laws and rules thereof of the Government of India as an endangered or threatened species restricting or regulating its collection and observation. Therefore, no permits were required.

References

Ahlawat S, Singh D, Yadav A, Singh AK, Virdi JS, Sharma KK (2020) Proteomic analysis reveals the damaging role of low redox laccase from *Yersinia enterocolitica* strain 8081 in the midgut of *Helicoverpa armigera*. Biotechnol Lett 42:2189–2210. https://doi.org/10.1007/s10529-020-02925-x

Alenizi D, Ringwood T, Redhwan A, Bouraha B, Wren BW, Prentice M, McNally A (2016) All *Yersinia enterocolitica* are pathogenic: virulence of phylogroup 1 *Y. enterocolitica* in a *Galleria mellonella* infection model. Microbiology 162:1379–1387. https://doi.org/10.1099/mic.0.000311

Arafah S, Rosso ML, Rehaume L, Hancock RE, Simonet M, Marceau M (2009) An iron-regulated LysR-type element mediates antimicrobial peptide resistance and virulence in *Yersinia pseudotuberculosis*. Microbiology 155(7):2168–2181. https://doi.org/10.1099/mic.0.026690-0

Baker MJ, Trevisan J, Bassan P, Bhargava R, Butler HJ, Dorling KM, Fielden PR, Fogarty SW, Fullwood NJ, Heys KA, Hughes C, Lasch P, Martin-Hirsch PL, Obinaju B, Sockalingum GD, Sulé-Suso J, Strong RJ, Walsh MJ, Wood BR, Gardner P, Martin FL (2014) Using fourier transform IR

spectroscopy to analyze biological materials. Nat Protoc 9:1771. https://doi.org/10.1038/nprot.2014.110

Balasubramaniam B, Vinitha T, Deepika S, JebaMercy G, VenkataKrishna LM, Balamurugan K (2019) Analysis of *Caenorhabditis elegans* phosphoproteome reveals the involvement of a molecular chaperone, HSP-90 protein during *Salmonella enteric* Serovar Typhi infection. Int J Biol Macromol 137:620–646

Baldridge G, Higgins L, Witthuhn B, Markowski T, Baldridge A, Armien A, Fallon A (2017) Proteomic analysis of a mosquito host cell response to persistent *Wolbachia* infection. Res Microbiol 168:609–625. https://doi.org/10.1016/j.ijbiomac.2019.06.085

Barnoy S, Gancz H, Zhu Y, Honnold CL, Zurawski DV, Venkatesan MM (2017) The *Galleria mellonella* larvae as an in vivo model for evaluation of *Shigella* virulence. Gut Microbes 8(4):335–350. https://doi.org/10.1080/19490976.2017.1293225

Bich L, Mossio M, Ruiz-Mirazo K, Moreno A (2016) Biological regulation: controlling the system from within. Biol Philos 31(2):237–265. https://doi.org/10.1007/s10539-015-9497-8

Brem D, Pelludat C, Rakin A, Jacobi CA, Heesemann J (2001) Functional analysis of yersiniabactin transport genes of *Yersinia enterocolitica*. Microbiology 147(5):1115–1127. https://doi.org/10.1099/00221287-147-5-1115

Campbell PM, Cao AT, Hines ER, East PD, Gordon KH (2008) Proteomic analysis of the peritrophic matrix from the gut of the caterpillar, *Helicoverpa armigera*. Insect Biochem Mol Biol 38:950–958. https://doi.org/10.1016/j.ibmb.2008.07.009

Cools F, Torfs E, Porto A, de Abreu J, Vanhoutte B, Maes L, Caljon G, Delputte P, Cappoen D, Cos P (2019) Optimization and characterization of a *Galleria mellonella* larval infection model for virulence studies and the evaluation of therapeutics against *Streptococcus pneumoniae*. Front Microbiol 10:311. https://doi.org/10.3389/fmicb.2019.00311

Cuéllar-Cruz M, Castaño I, Arroyo-Helguera O, De Las PA (2009) Oxidative stress response to menadione and cumene hydroperoxide in the opportunistic fungal pathogen *Candida glabrata*. Mem Inst Oswaldo Cruz 104:649–654. https://doi.org/10.1590/s0074-02762009000400020

Davis KM (2018) All *Yersinia* are not created equal: phenotypic adaptation to distinct niches within mammalian tissues. Front Cell Infect Microbiol 8:261. https://doi.org/10.3389/fcimb.2018.00261

Edelstein PH, Hu B, Shinzato T, Edelstein MA, Xu W, Bessman MJ (2005) *Legionella pneumophila* NudA Is a Nudix hydrolase and virulence factor. Infect Immun 73(10):6567. https://doi.org/10.1128/IAI.73.10.6567-6576.2005

Ganz T (2018) Iron and infection. Int J Hematol 107:7–15. https://doi.org/10.1007/s12185-017-2366-2

Garbom S, Forsberg Å, Wolf-Watz H, Kihlberg BM (2004) Identification of novel virulence-associated genes via genome analysis of hypothetical genes. Infect Immun 72(3):1333. https://doi.org/10.1128/IAI.72.3.1333-1340.2004

Hering NA, Fromm A, Kikhney J, Lee IM, Moter A, Schulzke JD, Bücker R (2016) *Yersinia enterocolitica* affects intestinal barrier function in the colon. J Infect Dis 213:1157–1162. https://doi.org/10.1093/infdis/jiv571

Hurst MR, Beattie AK, Jones SA, Hsu PC, Calder J, van Koten C (2015) Temperature-dependent *Galleria mellonella* mortality as a result of *Yersinia entomophaga* infection. Appl Environ Microbiol 81:6404–6414. https://doi.org/10.1128/AEM.00790-15

Inguglia L, Chiaramonte M, Arizza V, Turiák L, Vékey K, Drahos L, Pitonzo R, Avellone G, Stefano VD (2020) Changes in the proteome of sea urchin *Paracentrotus lividus* coelomocytes in response to LPS injection into the body cavity. PLoS ONE 15:e0228893. https://doi.org/10.1371/journal.pone.0228893

Insua JL, Llobet E, Moranta D, Pérez-Gutiérrez C, Tomás A, Garmendia J, Bengoechea JA (2013) Modeling *Klebsiella pneumoniae* pathogenesis by infection of the wax moth *Galleria mellonella*. Infect Immun 81:3552–3565. https://doi.org/10.1128/IAI.00391-13

Jakubowska AK, Caccia S, Gordon KH, Ferré J, Herrero S (2010) Downregulation of a chitin deacetylase-like protein in response to baculovirus infection and its application for improving baculovirus infectivity. J Virol 84:2547–2555. https://doi.org/10.1128/JVI.01860-09

Jain KK, Kumar A, Shankar A, Pandey D, Chaudhary B, Sharma KK (2019) De novo transcriptome assembly and protein profiling of copper-induced lignocellulolytic fungus *Ganoderma lucidum* MDU-7 reveals genes involved in lignocellulose degradation and terpenoid biosynthetic pathways. Genomics 112:184–198. https://doi.org/10.1016/j.ygeno.2019.01.012

Krachler AM, Sirisaengtaksin N, Monteith P, Paine CT, Coates CJ, Lim J (2021) Defective phagocyte association during infection of *Galleria mellonella* with *Yersinia pseudotuberculosis* is detrimental to both insect host and microbe. Virulence 12(1):638–653. https://doi.org/10.1080/21505594.2021.1878672

Kumar V, Bal A, Gill KD (2008) Impairment of mitochondrial energy metabolism in different regions of rat brain following chronic exposure to aluminium. Brain Res 232:94–103. https://doi.org/10.1016/j.brainres.2008.07.028

Kurutas EB (2016) The importance of antioxidants which play the role in cellular response against oxidative/nitrosative stress: current state. J Nutr 15:71. https://doi.org/10.1186/s12937-016-0186-5

Lee KS, Kim SR, Park NS, Kim I, Kang PD, Sohn BH (2005) Characterization of a silkworm thioredoxin peroxidase that is induced by external temperature stimulus and viral infection. Insect Biochem Mol Biol 35:73–84. https://doi.org/10.1016/j.ibmb.2004.09.008

Li X, Liu Q, Lewis EE, Tarasco E (2016) Activity changes of antioxidant and detoxifying enzymes in *Tenebrio molitor* (Coleoptera: Tenebrionidae) larvae infected by the entomopathogenic nematode *Heterorhabditis beicherriana* (Rhabditida: Heterorhabditidae). Parasitol Res 115:4485–4494. https://doi.org/10.1007/s00436-016-5235-7

Lü D, Xu P, Hou C, Gao K, Guo X (2019) Label-free LC-MS/MS proteomic analysis of the hemolymph of silkworm larvae infected with *Beauveria bassiana*. J Invertebr Pathol 166:107227. https://doi.org/10.1016/j.jip.2019.107227

Manjunatha GKS, Peter A, Naika MB, Niranjana P, Shamprasad P (2018) Identification of in-vitro red fluorescent protein with antipathogenic activity from the midgut of the silkworm (*Bombyx mori L.*). Protein Pept Lett 25:302–313. https://doi.org/10.2174/0929866525666180115121853

Manrique M, Pareja-Tobes P, Pareja-Tobes E, Pareja E, Tobes R (2011) *Escherichia coli* EHEC Germany outbreak preliminary functional annotation using BG7 system. Nat Preced. https://doi.org/10.1038/npre.2011.6001.1

Marzban R, He Q, Zhang Q, Liu XX (2013) Histopathology of cotton bollworm midgut infected with *Helicoverpa armigera* cytoplasmic polyhedrosis virus. Braz J Microbiol 44:1231–1236. https://doi.org/10.1590/s1517-83822013000400029

McQuade R, Stock SP (2018) Secretion systems and secreted proteins in Gram-negative entomopathogenic bacteria: their roles in insect virulence and beyond. Insects 9:68. https://doi.org/10.3390/insects9020068

Mir DA, Balamurugan K (2019) A proteomic analysis of *Caenorhabditis elegans* mitochondria during bacterial infection. Mitochondrion 48:37–50. https://doi.org/10.1016/j.mito.2019.03.002

Nappi AJ, Christensen BM (2005) Melanogenesis and associated cytotoxic reactions: applications to insect innate immunity. Insect Biochem Mol Biol 35:443–459. https://doi.org/10.1016/j.ibmb.2005.01.014

Pereira MF, Rossi CC, de Queiroz MV, Martins GF, Isaac C, Bosse JT, Li Y, Wren BW, Terra VS, Cuccui J, Langford PR, Bazzolli DMS (2015) *Galleria mellonella* is an effective model to study *Actinobacillus pleuropneumoniae* infection. Microbiology 161:387–400. https://doi.org/10.1099/mic.0.083923-0

Perez-Riverol Y, Csordas A, Bai J, Bernal-Llinares M, Hewapathirana S, Kundu DJ, Inuganti A, Griss J, Mayer G, Eisenacher M, Pérez E, Uszkoreit J, Pfeuffer J, Sachsenberg T, Yilmaz S, Tiwary S, Cox J, Audain E, Walzer M, Jarnuczak AF, Ternent T, Brazma A, Vizcaíno JA (2019) The PRIDE database and related tools and resources in 2019: improving support for quantification data. Nucleic Acids Res 47(D1):D442–D450. https://doi.org/10.1093/nar/gky1106

Rajendran P, Nandakumar N, Rengarajan T, Palaniswami R, Gnanadhas EN, Lakshminarasaiah U, Gopas J, Nishigaki I (2014) Antioxidants and human diseases. Clin Chim Acta 436:332–347. https://doi.org/10.1016/j.cca.2014.06.004

Rakin A, Garzetti D, Bouabe H, Sprague LD (2015) Yersinia enterocolitica. In: Tang YW, Sussman M, Liu D, Poxton I, Schwartzman J (eds) Molecular medical microbiology. Academic Press, New York, pp 1319–1344

Schubert KA, Xu Y, Shao F, Auerbuch V (2020) The *Yersinia* type III secretion system as a tool for studying cytosolic innate immune surveillance. Ann Rev Microbiol 74:221–245. https://doi.org/10.1146/annurev-micro-020518-120221

Senior NJ, Bagnall MC, Champion OL, Reynolds SE, La Ragione RM, Woodward MJ, Salguero FJ, Titball RW (2011) *Galleria mellonella* as an infection model for *Campylobacter jejuni* virulence. J Med Microbiol 60:661–669. https://doi.org/10.1099/jmm.0.026658-0

Singh D, Sharma KK, Dhar MS, Virdi JS (2014) Molecular modeling and docking of novel laccase from multiple serotype of *Yersinia enterocolitica* suggests differential and multiple substrate binding. Biochem Biophys Res Commun 449:157–162. https://doi.org/10.1016/j.bbrc.2014.05.003

Singh D, Rawat S, Waseem M, Gupta S, Lynn A, Nitin M, Ramchiary N, Sharma KK (2016) Molecular modeling and simulation studies of recombinant laccase from *Yersinia enterocolitica* suggests significant role in the biotransformation of non-steroidal anti-inflammatory drugs. Biochem Biophys Res Commun 469:306–312. https://doi.org/10.1016/j.bbrc.2015.11.096

Springer K, Sänger PA, Moritz C, Felsl A, Rattei T, Fuchs TM (2018) Insecticidal toxicity of *Yersinia* species involves the novel enterotoxin YacT. Front Cell Infect Microbiol 8:392. https://doi.org/10.3389/fcimb.2018.00392

Tang T, Yang Z, Li J, Yuan F, Xie S, Liu F (2019) Identification of multiple ferritin genes in *Macrobrachium nipponense* and their involvement in redox homeostasis and innate immunity. Fish Shellfish Immunol 89:701–709. https://doi.org/10.1016/j.fsi.2019.04.050

Thomson NR, Howard S, Wren BW, Holden MT, Crossman L, Challis GL, Churcher C, Mungall K, Brooks K, Chillingworth T, Feltwell T, Abdellah Z, Hauser H, Jagels K, Maddison M, Moule S, Sanders M, Whitehead S, Quail MA, Dougan G, Parkhill J, Prentice MB (2006) The complete genome sequence and comparative genome analysis of the high pathogenicity *Yersinia enterocolitica* strain 8081. PLoS Genet 2:e206. https://doi.org/10.1371/journal.pgen.0020206

Tsai CJY, Loh JMS, Proft T (2016) *Galleria mellonella* infection models for the study of bacterial diseases and for antimicrobial drug testing. Virulence 7:214–229. https://doi.org/10.1080/21505594.2015.1135289

Von Pawel-Rammingen U, Telepnev MV, Schmidt G, Aktories K, Wolf-Watz H, Rosqvist R (2000) GAP activity of the *Yersinia* YopE cytotoxin specifically targets the Rho pathway: a mechanism for disruption of actin microfilament structure. Mol Microbiol 36:737–748. https://doi.org/10.1046/j.1365-2958.2000.01898.x

Virdi JS, Kumar P, Mallik S, Bhagat N, Gulati P (2012) Insights into the genetic relationships between environmental and clinical strains of *Yersinia enterocolitica* Biovar 1A. In: Satyanarayana T, Johri BN, Prakash A (eds) Microorganisms in environmental management: microbes and environment. Springer, Dordrecht, pp 61–80

Wills ED (1966) Mechanisms of lipid peroxide formation in animal tissues. Biochem J 99:667–676. https://doi.org/10.1042/bj0990667

Wu HD, Liu QZ (2012) Antioxidative responses in *Galleria mellonella* larvae infected with the entomopathogenic nematode *Heterorhabditis* sp. *beicherriana*. Biocontrol Sci Technol 22:601–606. https://doi.org/10.1080/09583157.2012.670803

Yuan C, Xing L, Wang M, Wang X, Yin M, Wang Q, Hu Z, Zou Z (2017) Inhibition of melanization by serpin-5 and serpin-9 promotes baculovirus infection in cotton bollworm *Helicoverpa armigera*. PLoS Pathog 13:e1006645. https://doi.org/10.1371/journal.ppat.1006645

Zhang X, Guo W (2011) Isolation and identification of insect intestinal mucin haiim86-the new target for *Helicoverpa*

armigera biocontrol. Int J Biol Sci 7:286. https://doi.org/10.7150/ijbs.7.286

Zhang Y, Xia D, Zhao Q, Zhang G, Zhang Y, Qiu Z, Shen D, Lu C (2019) Label-free proteomic analysis of silkworm midgut infected by *Bombyx mori* nuclear polyhedrosis virus. J Proteom 200:40–50. https://doi.org/10.1016/j.jprot.2019.03.011

Publisher's Note Springer Nature remains neutral with regard to jurisdictional claims in published maps and institutional affiliations.